Available online at www.sciencedirect.com
ScienceDirect
Icarus 194 (2008) 125–136
ICARUS
www.elsevier.com/locate/icarus

V-type asteroids in the middle main belt ☆

F. Roig [a,*], D. Nesvorný [b,1], R. Gil-Hutton [c], D. Lazzaro [a]

[a] *Observatório Nacional, Rua Gal. José Cristino 77, Rio de Janeiro, RJ 20921-400, Brazil*
[b] *Southwest Research Institute, 1050 Walnut Street, Boulder, CO 80302, CO, USA*
[c] *Complejo Astronómico El Leoncito and Universidad Nacional de San Juan, Av. España 1512 sur, San Juan, J5402DSP, Argentina*

Received 5 July 2007; revised 15 October 2007

Available online 4 December 2007

Abstract

V-type asteroids are bodies whose surfaces are constituted of basalt. In the Main Asteroid Belt, most of these asteroids are assumed to come from the basaltic crust of Asteroid (4) Vesta. This idea is mainly supported by (i) the fact that almost all the known V-type asteroids are in the same region of the belt as (4) Vesta, i.e., the inner belt (semi-major axis $2.1 < a < 2.5$ AU), (ii) the existence of a dynamical asteroid family associated to (4) Vesta, and (iii) the observational evidence of at least one large craterization event on Vesta's surface. One V-type asteroid that is difficult to fit in this scenario is (1459) Magnya, located in the outer asteroid belt, i.e., too far away from (4) Vesta as to have a real possibility of coming from it. The recent discovery of the first V-type asteroid in the middle belt ($2.5 < a < 2.8$ AU), (21238) 1995WV7 [Binzel, R.P., Masi, G., Foglia, S., 2006. Bull. Am. Astron. Soc. 38, 627; Hammergren, M., Gyuk, G., Puckett, A., 2006. ArXiv e-print, astro-ph/0609420], located at ∼2.54 AU, raises the question of whether it came from (4) Vesta or not. In this paper, we present spectroscopic observations indicating the existence of another V-type asteroid at ∼2.53 AU, (40521) 1999RL95, and we investigate the possibility that these two asteroids evolved from the Vesta family to their present orbits by a semi-major axis drift due to the Yarkovsky effect. The main problem with this scenario is that the asteroids need to cross the 3/1 mean motion resonance with Jupiter, which is highly unstable. Combining N-body numerical simulations of the orbital evolution, that include the Yarkovsky effect, with Monte Carlo models, we compute the probability that an asteroid of a given diameter D evolves from the Vesta family and crosses over the 3/1 resonance, reaching a stable orbit in the middle belt. Our results indicate that an asteroid like (21238) 1995WV7 has a low probability (∼1%) of having evolved through this mechanism due to its large size ($D \sim 5$ km), because the Yarkovsky effect is not sufficiently efficient for such large asteroids. However, the mechanism might explain the orbits of smaller bodies like (40521) 1999RL95 ($D \sim 3$ km) with ∼70–100% probability, provided that we assume that the Vesta family formed $\gtrsim$3.5 Gy ago. We estimate the debiased population of V-type asteroids that might exist in the same region as (21238) and (40521) ($2.5 < a \lesssim 2.62$ AU) and conclude that about 10 to 30% of the V-type bodies with $D > 1$ km may come from the Vesta family by crossing over the 3/1 resonance. The remaining 70–90% must have a different origin.

Keywords: Asteroids, composition; Asteroids, dynamics

1. Introduction

The recent discovery of (21238) 1995WV7 (Binzel et al., 2006; Hammergren et al., 2006), a basaltic asteroid in the middle main belt ($2.5 < a < 2.82$ AU), raised new questions about the origin of basaltic material in the asteroid belt.

Basaltic asteroids show a spectrum characterized by the presence of a deep absorption band centered at ∼0.9 μm, and are classified as V-type in the usual taxonomies (Tholen, 1989; Bus and Binzel, 2002a). Most of the known V-type asteroids seem to be fragments from the crust of Asteroid (4) Vesta.

☆ Based on observations obtained at the Gemini Observatory, which is operated by the Association of Universities for Research in Astronomy, Inc., under a cooperative agreement with the NSF on behalf of the Gemini partnership: the National Science Foundation (USA), the Particle Physics and Astronomy Research Council (UK), the National Research Council (Canada), CONICYT (Chile), the Australian Research Council (Australia), CNPq (Brazil) and CONICET (Argentina), Program ID: GS-2006A-Q51.

* Corresponding author.
E-mail address: froig@on.br (F. Roig).

[1] Visiting scientist, Observatório Nacional, Rio de Janeiro, Brazil.

0019-1035/$ – see front matter
doi:10.1016/j.icarus.2007.10.004

This is supported by the fact that (4) Vesta is the only large asteroid showing a basaltic crust (McCord et al., 1970), and almost all V-type asteroids are found in the same region of the main belt as Vesta, i.e., the inner belt ($a < 2.5$ AU). Moreover, (4) Vesta has associated a dynamical asteroid family, the Vesta family, whose members are also V-type (Mothé-Diniz et al., 2005) and most probably originated from the excavation of a large crater on Vesta's surface (Thomas et al., 1997; Asphaug, 1997).

The discovery of (1459) Magnya (Lazzaro et al., 2000), a V-type asteroid in the outer belt ($a > 2.82$ AU), provided the first evidence for another possible source of basaltic asteroids in the main belt. (1459) Magnya is too far away from the Vesta region as to have any chance of being a fragment from Vesta's crust. No dynamical mechanism is known to be able to bring an asteroid from the Vesta family to the Magnya region. Moreover, Magnya is too big (diameter $D \sim 17$ km) as to fit within the size distribution of the Vesta family (see Section 4). Michtchenko et al. (2002) suggested that Magnya is the fragment from a differentiated parent body that broke up in the outer belt, but up to now no other V-type asteroids have been confirmed in the same region of the belt to support this hypothesis (Duffard and Roig, 2007; Moskovitz et al., 2007).

The case of (21238) 1995WV7, the first V-type asteroid discovered in the middle belt, has some similarities with the case of Magnya, but also shows some differences. (21238) 1995WV7 is also far away from Vesta, and unrealistic ejection velocities larger than ∼2 km/s would be necessary to directly transport it form Vesta's surface to its present orbit. These ejection velocities cannot be produced in typical craterization events similar to the one that originated the Vesta family (Asphaug, 1997). On the other hand, (21238) 1995WV7 is close to the outer border of the 3/1 mean motion resonance with Jupiter (hereafter J3/1 MMR), centered at 2.5 AU, and its size ($D \sim 5$ km) fits within the size distribution of the Vesta family. Since the inner border of the J3/1 MMR is very close to the outer edge of the Vesta family, the possibility of (21238) 1995WV7 being a former member of this family that reached its present orbit after crossing over the resonance cannot be totally ruled out. The J3/1 MMR is highly chaotic (Wisdom, 1982) and is considered a difficult-to-cross barrier, but up to now no detailed studies have been made to confirm this.

A different scenario is proposed by Carruba et al. (2007a), in which the source for (21238) 1995WV7 and other, yet undiscovered, basaltic asteroids in the middle belt could be Asteroid (15) Eunomia located at $a \sim 2.65$ AU. This asteroid appears to be partially differentiated, showing a mineralogical composition in part of its surface that might indicate the previous existence of a basaltic crust (Nathues et al., 2005). Carruba et al. suggest that several collisions made (15) Eunomia lose its basaltic crust almost completely, and the subsequent fragments were significantly dispersed in the middle belt over the age of the Solar System.

The aim of this work is to study the possible origin of (21238) 1995WV7 and other V-type asteroids in the middle asteroid belt. In particular, we analyze the possibility that asteroids from the Vesta family increase their orbital semi-major axis due to the Yarkovsky effect (Vokrouhlický et al., 2000) and cross the J3/1 MMR, reaching stable orbits in the middle belt. In Section 2, we introduce the population of V-type asteroids observed by the Sloan Digital Sky Survey in the middle belt, and present our spectroscopic observations with the Gemini South Telescope that allow to confirm another V-type asteroid in the same region as (21238). In Section 3, we describe our simulations, analyze the resonance crossing mechanism proposed above, and evaluate its efficiency to produce V-type asteroids beyond 2.5 AU. In Section 5, we discuss our results compared to the debiased distribution of V-type asteroids in the middle belt. Finally, Section 6 is devoted to the conclusions.

2. V-type asteroids in the middle belt

The existence of V-type asteroids in the middle belt was first suggested by Roig and Gil-Hutton (2006), who analyzed the colors of the Sloan Digital Sky Survey Moving Objects Catalog (SDSS-MOC; Ivezic et al., 2001). These authors studied a sample of 13,290 asteroids contained in the 3rd release of the SDSS-MOC that exhibit small photometric errors (less than 10%) in all the five bands of the SDSS photometric system, named u, g, r, i, z, respectively. They found three candidate V-type asteroids in the middle belt, which are listed in Table 1. Two of them are located very close to the outer border of the J3/1 MMR. The third one is close to the outer border of the J8/3 MMR, centered at 2.7 AU. The spectroscopic confirmation of the basaltic nature of (21238) was reported by Binzel et al. (2006), based on spectroscopic observations in the near infrared (NIR), and also by Hammergren et al. (2006) based on visible spectroscopic plus NIR photometry.

As part of an observational campaign to confirm the taxonomy of V-type candidates identified by Roig and Gil-Hutton (2006), we obtained spectra of (21238) and (40521) in the visible. The observations were carried out during the nights of 29–30 April, 2006, at the Gemini South Observatory (GS), using the Gemini Multi-Object Spectrograph (GMOS). Table 2 provides the observational circumstances of the targets. In order to remove the solar signature from the asteroids spectra, we also observed the stars SA 107-871 ($V = 12.4$) and SA 110-361

Table 1
Proper semi-major axis a_p, proper eccentricity e_p, sin of proper inclination $\sin I_p$, absolute magnitude H and diameter D of predicted V-type asteroids in the middle belt according to the colors of the SDSS-MOC

Name	a_p [AU]	e_p	$\sin I_p$	H	D [km]
(21238) 1995WV7	2.54108	0.1371	0.1866	13.04	5.15
(40521) 1999RL95	2.53111	0.0458	0.2159	14.36	2.80
(66905) 1999VC160	2.74627	0.1457	0.2291	14.51	2.62

Diameters have been estimated assuming an albedo of 0.4, typical of basaltic asteroids: 0.42 for (4) Vesta (Tedesco, 1989) and 0.37 for (1459) Magnya (Delbo et al., 2006).

Table 2
Observational circumstances of (21238) and (40521): Δ is geocentric distance in AU, r is heliocentric distance in AU, ϕ is solar phase angle, θ is solar elongation, V is visible magnitude

Asteroid	Date [UT]	α (J2000)	δ (J2000)	Δ	r	ϕ	θ	V
(21238)	2006 Apr 29.4094	$20^h44^m53.01^s$	$-24°57'12.8''$	2.599	2.818	20.9°	91.9°	18.3
(40521)	2006 Apr 30.2811	$14^h11^m29.86^s$	$-24°01'44.8''$	1.489	2.487	4.1°	169.8°	18.1

Dates correspond to the starting time of the observations. The observing conditions were better than 85% of image quality, 70% of sky transparency (cloud cover), 100% of sky transparency (water vapor), 80% of sky background, air mass <1.5.

Table 3
Number of exposures, exposure times (individual and total), S/N at 0.90 μm of the raw and rebinned spectra, and solar analog used in the reduction

Asteroid	n_{exp}	T_{exp}	T_{total}	S/N (raw)	S/N (rebinned)	Solar analog
(21238)	6	200 s	1200 s	20	80	SA 110-361
(40521)	6	500 s	3000 s	18	72	SA 107-871

($V = 12.4$), taken from the selected areas of Landolt (1992), that we used as solar analog stars.[2]

Tracking of the asteroids at non-sidereal rate was not possible because the use of the peripherical Wavefront Sensor (WFS) is not recommended due to flexure within GMOS. Instead, we used the On-Instrument Wavefront Sensor (OIWFS) tracking at sidereal rate, with the slit oriented in the direction of the asteroid's proper motion.

All the observations were performed using the following GMOS configuration: grating R400, filter OG515 to avoid second order spectrum contamination longwards of ∼0.7 μm, slit width 1.5 arcsec (the maximum allowable with GS-GMOS), central wavelength 0.73 μm, spectral coverage 0.522 to 0.938 μm, spatial binning 2, and spectral binning 4. This configuration provides a resolution $R \sim 3\,000$ at 0.90 μm, but $R \sim 200$ is enough to detect the deep absorption band longwards of 0.75 μm typical of V-type spectra. Therefore, it was possible to do a 15:1 rebinning of the asteroids spectra to improve the final signal-to-noise (S/N) ratio by a factor of ∼4.

Each asteroid was observed six times at six different positions along the slit separated by 10 arcsec. Each solar analog star was observed three times at three different positions along the slit with the same separation. The integration times for the asteroids allowed to attain S/N ∼20 at 0.90 μm which, after spectral rebinning, provided a minimum S/N ∼70. Table 3 summarizes the asteroids exposure times. The exposure times for the solar analog stars were chosen to reach 50–70% of the detector full well (100k electrons) per exposure. Wavelength calibration of the spectra was performed using a standard CuAr lamp.

The GMOS IRAF package was used to perform the standard reduction tasks. Since each image was dithered along the spatial direction, we remove the fringes by making a background image resulting from the combination of three successive images centered around the time of the image we want to correct. After the fringe correction, the individual frames were coadded to improve the S/N and the spectrum was extracted.

The final spectra of (21238) and (40521) are shown in Fig. 1. We have plot in gray several spectra of known V-type asteroids taken from the SMASS (Bus and Binzel, 2002b) and S^3OS^2 (Lazzaro et al., 2004) surveys for comparison. Both spectra are compatible with the V class, showing the typical absorption band with a minimum at 0.90 μm. Our observations with Gemini constitute another independent confirmation of the basaltic nature of (21238), and also allow the confirmation of (40521) as the second V-type asteroid found in the middle belt.[3] Fig. 2 compares the observed spectra to the SDSS-MOC colors (gray dots) showing the good agreement between both data sets.

3. Possible origin of V-type asteroids in the middle belt

In the following, we analyze the possibility that (21238) and (40521) were fragments of (4) Vesta that evolved to their current orbits by the Yarkovsky effect (for a description of this effect see Bottke et al., 2006). The main problem with this scenario is that these asteroids needed to cross the J3/1 MMR which is notably unstable. To estimate the time Δt_{cross} that a 5 km asteroid would require to cross the J3/1 MMR, Hammergren et al. (2006) divided the resonance width Δa by the drift rate da/dt due to the Yarkovsky effect, and concluded that $\Delta t_{cross} \gg t_{inst}$, where t_{inst} is the instability time scale of the J3/1 MMR (i.e., the time required for a population of asteroids to be removed from the resonance, see Gladman et al., 1997). These authors thus inferred that it would be impossible for an asteroid like (21238) to cross the J3/1 MMR. However, this argument is only approximative because it does not take into account the resonance dynamics. Here we used precise N-body numerical simulations to study whether the crossing is actually possible and *how does this depend on the drift rate* da/dt.

We performed a series of simulations of the evolution of test particles representing selected members of the Vesta dynamical family. To define this family, we used the database of 188,207 asteroid proper elements released by March 2005 (AstDys, http://hamilton.dm.unipi.it/cgi-bin/astdys/astibo). This database is contemporary to the 3rd release of the SDSS-MOC, therefore the two datasets can be directly compared. We applied the Hierarchical Clustering Method (HCM; Zappalà et al., 1990) and defined the Vesta family at a cutoff of 60 m/s,

[2] These are G2V stars with solar colors, and in the magnitude range allowed by Gemini telescopes ($V > 11$). We recall that no spectroscopic solar analog stars are available in the literature in this magnitude range.

[3] The ASCII files of the spectra are available at http://staff.on.br/froig/vtypes.

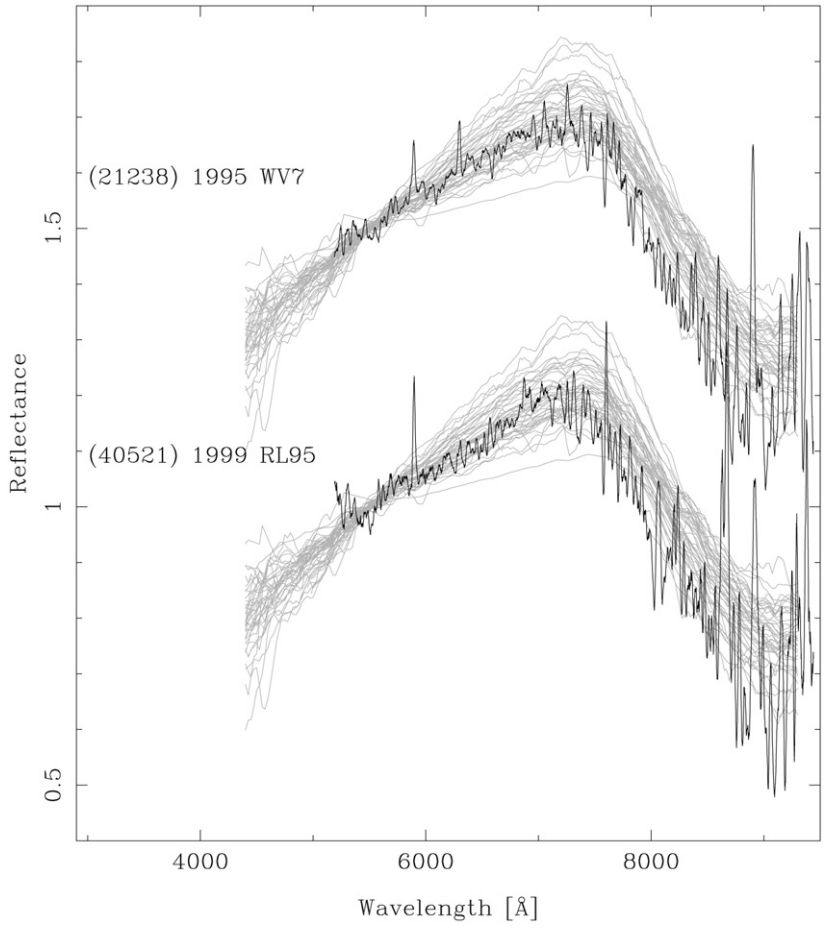

Fig. 1. Visible spectra of (21238) and (40521) observed with GMOS at Gemini South (black lines). The gray lines are the spectra of other known V-type asteroids. The spectra are normalized to 1 at 5500 Å and shifted by 0.5 in reflectance for clarity. A running box of 20 Å has been applied to smooth the spectra.

which is 5 m/s larger than the computed quasi-random level (i.e., the average minimum distance between pairs of neighbor asteroids) for the inner belt. This guaranteed that we defined the Vesta family with the largest possible number of members (we found ∼9 500) that could be detected from the given dataset of proper elements.

Among the members of the Vesta family, we selected 21 asteroids with $2.485 \leqslant a_p \leqslant 2.490$ AU, which are the closest ones to the J3/1 MMR, and generated 100 clones of each, i.e., 2100 bodies in total. All 100 clones had the same orbital parameters as the original asteroid, but we allowed each to drift in semi-major axis at a slightly different rate $\mathrm{d}a/\mathrm{d}t > 0$ due to the Yarkovsky effect. In this way the clones reached the border of the J3/1 MMR at different phases of the resonant angle $\sigma = 3\lambda_\mathrm{J} - \lambda - \varpi$, where λ_J, λ are the mean longitudes of Jupiter and the asteroid, respectively, and ϖ is the longitude of perihelion of the asteroid. Therefore, they sampled different resonant interaction histories.

The simulations were performed using a modified version of the SWIFT_MVS integrator (Levison and Duncan, 1994). The bodies were considered as massless particles subject to perturbations from all planets except Mercury, and the Yarkovsky effect was introduced in the simulation as an additional acceleration term depending on the velocity as

$$\left(\frac{\mathrm{d}^2\vec{r}}{\mathrm{d}t^2}\right)_{\mathrm{Yarko}} = \frac{GM}{2a^2}\frac{\mathrm{d}a}{\mathrm{d}t}\frac{\vec{v}}{v^2},$$

where G is the gravitational constant, M the mass of the Sun, a the osculating semi-major axis of the orbit, $\vec{r}$, $\vec{v}$ the instantaneous position and velocity of the body, and $\mathrm{d}a/\mathrm{d}t$ the required drift rate measured in AU/y. According to the analytical theory of Vokrouhlický (1999), the diurnal Yarkovsky drift rate approximately scales with diameter as

$$\frac{\mathrm{d}a}{\mathrm{d}t} \simeq 2.5 \times 10^{-4}\ \mathrm{AU\,My^{-1}}\,\frac{1\ \mathrm{km}}{D}\cos\epsilon, \tag{1}$$

where D is in km, ϵ is the spin axis obliquity, and the coefficient was obtained assuming physical and thermal parameters typical of basalt and albedo 0.4 [see Nesvorný et al. (2008) for details]. We chose the thermal parameters to produce large but plausible drift rates, because this would favor the J3/1 MMR crossing. Slower drift rates would apply if the real thermal parameters have different values. The so-called seasonal Yarkovsky effect (Rubincam, 1995) was not included in our model because it only produces $\mathrm{d}a/\mathrm{d}t < 0$ (i.e., a drift away from the resonance) and it is an order of magnitude smaller than the diurnal effect modeled by Eq. (1) for km-size asteroids. Effects of spin axis reorientation, like collisions (Harris, 1979) or the YORP effect

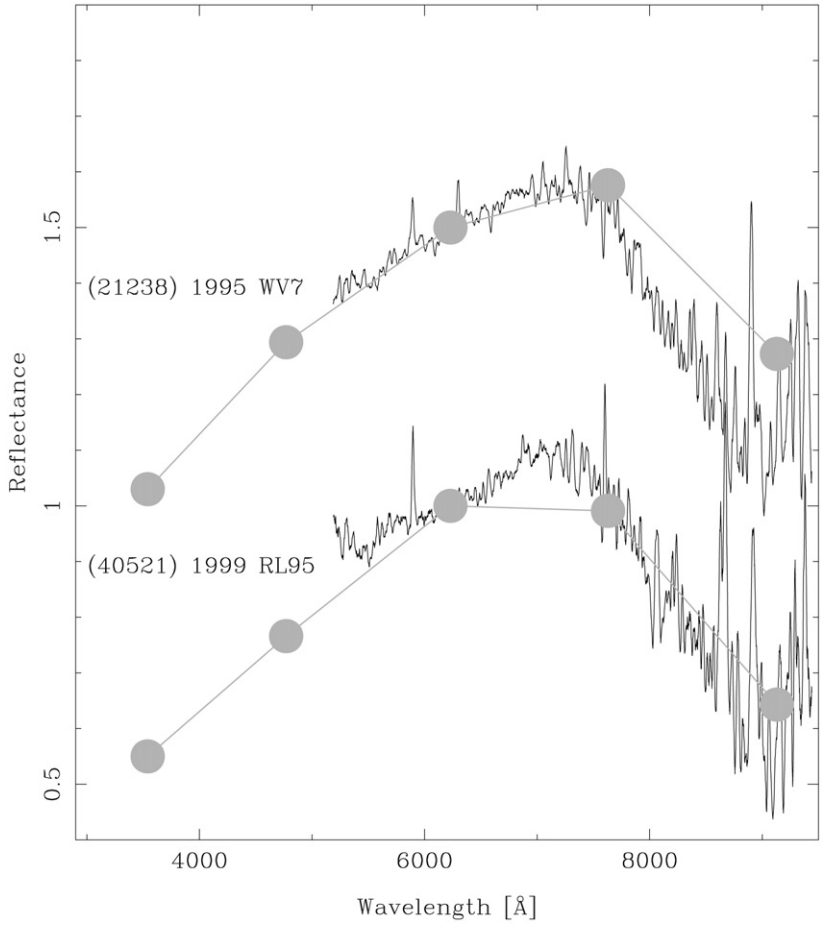

Fig. 2. Visible spectra of (21238) and (40521) (black lines) compared to the SDSS-MOC fluxes (gray dots). The spectra are normalized to 1 at 6230 Å (i.e., the center of the r band) and shifted by 0.5 in reflectance for clarity. The size of the dots gives an idea of the errors involved.

(Rubincam, 2000), were not taken into account either because they are not relevant for this numerical experiment: only the drift rate matters.

We performed three series of simulations. In the first series, we assumed that each clone drifted outwards at a rate randomly chosen in the interval $(1.0 \pm 0.1) \times 10^{-4}$ AU/My, that according to Eq. (1) corresponds to $D \sim 2.5$ km V-type asteroids. The interval ± 0.1 allows the clones to sample different times of arrival to the border of the J3/1 MMR and thus a wide range of resonant phases as discussed above.[4] These simulations spanned 150 My.

In the second series, the clones drifted at a rate randomly chosen in the interval $(2.5 \pm 0.25) \times 10^{-4}$ AU/My, which corresponds to $D \sim 1$ km asteroids. These simulations spanned 80 My. Finally, in the third series the drift rates were set in the interval $(1.0 \pm 0.1) \times 10^{-3}$ AU/My ($D \sim 250$ m), and these simulations spanned 25 My. The time step of the integrator was set to be 0.04 y.

In all the three simulations, more than ∼97% of the particles were discarded because they entered the J3/1 MMR and chaotically evolved to planet crossing orbits in a few My. These particles were eliminated by close encounters with the planets, mainly the Earth and Mars, or by impacting the Sun. But a small fraction—less than ∼3%—of the particles crossed over the J3/1 MMR and ended the simulation in apparently stable orbits with $a > 2.5$ AU.[5]

Fig. 3 shows two examples of test particles that crossed over the J3/1 MMR. The left panels correspond to a slowly drifting particle and the right panels correspond to a faster drift. The particles enter the J3/1 MMR at the side of lower semi-major axes, perform a few librations around the resonant semi-major axis, and exit the resonance at the side of larger semi-major axes. The particles remain in the resonance for at most a few 10^4 y. Their eccentricities and inclinations are not significantly affected by the passage through the resonance. In the examples shown in Fig. 3, the eccentricities decay to lower values but this happens *after* the particles have already crossed the J3/1 MMR. This effect is probably due to the interplay with several

[4] The different values of the Yarkovsky drift in this interval may be interpreted as caused either by slightly different properties (e.g., thermal conductivity) of the bodies' surfaces, or by slightly different orientations of the spin axes.

[5] "Stable orbit" means that the orbit is expected to remain in the middle belt in spite of eventual interactions with non-linear secular resonances located in the region close the border of the J3/1 MMR.

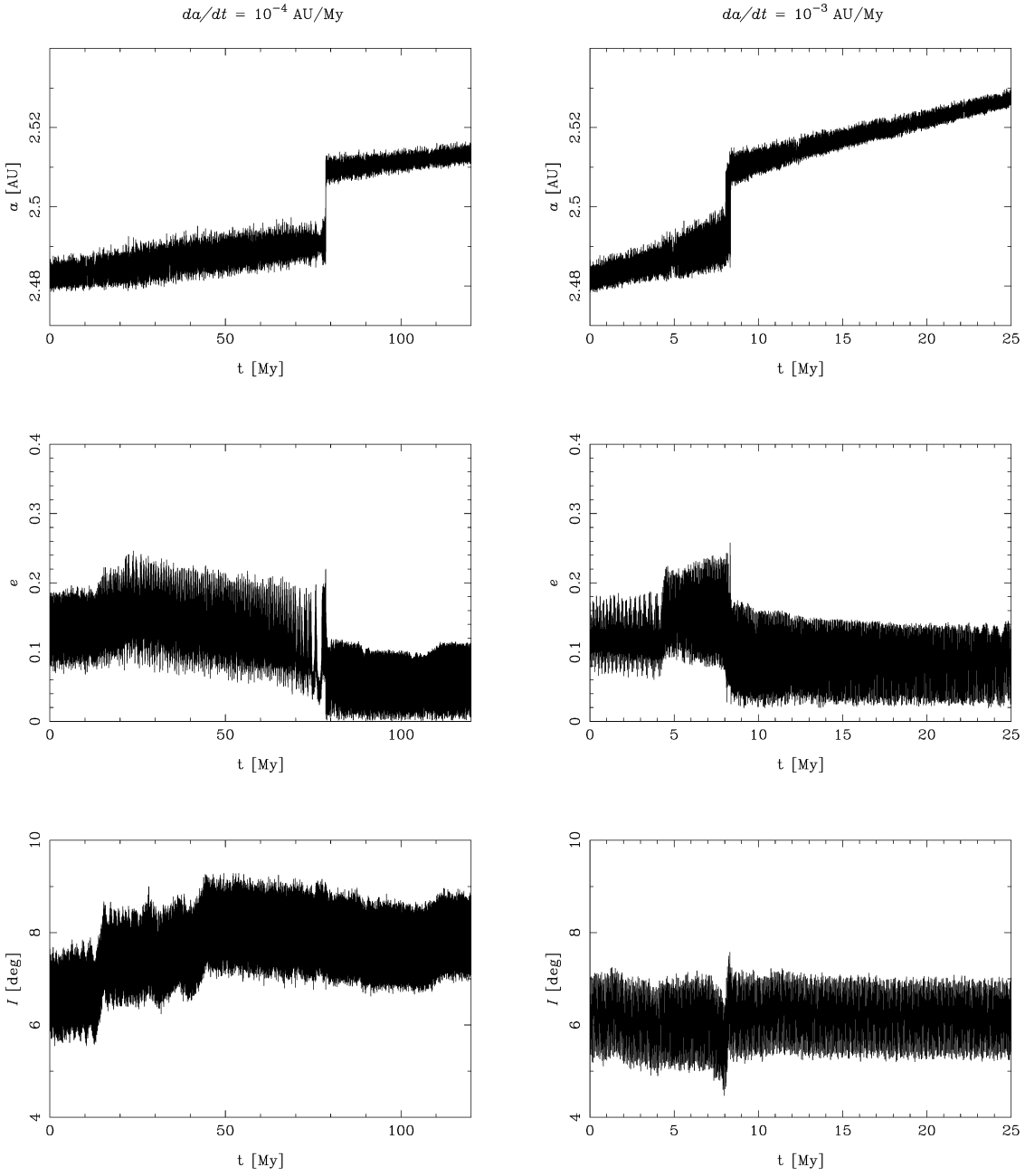

Fig. 3. Evolution of the semi-major axis, eccentricity and inclination of two test particles crossing over the J3/1 MMR at two different Yarkovsky drift rates. Note the different scales in the time axis.

non-linear secular resonances located close to the border of the J3/1 MMR, like the $g - 2g_6 + g_5$ resonance, where g is the secular frequency of the asteroid perihelion, and g_5, g_6 are the frequencies of the perihelia of Jupiter and Saturn, respectively. In general, the particles that jumped the J3/1 MMR ended the simulations either with higher or lower values of the eccentricities and inclinations than their original values.

In Fig. 4 we show the trajectory of the slowly drifting particle of Fig. 3 at the exact moment at which it crosses the J3/1 MMR. We can see that the particle spent only ∼5 000 y inside the resonance (top panel), so it virtually "jumps" over the resonance. The numbers in the bottom panel provide the temporal sequence of the trajectory. The particle enters the resonance somewhere between "1" and "2," then it performs one and a half libration sticking close to the resonance separatrix, and finally exits the resonance somewhere between "8" and "9." This trajectory is a typical example of the resonance crossing mechanism. We conjecture that only the orbits that remain close to the separatrix would be able to exit the resonance pushed by the Yarkovsky drift, and this might depend on the particular phase of the resonant angle, σ, that the orbit has when it enters the resonance.

From our simulations, it was possible to estimate the fraction of test particles that crossed the J3/1 MMR, $f_{\rm cross}$, and its formal uncertainty, as a function of the Yarkovsky drift rate. The results are given in Table 4. Assuming that these results reflect

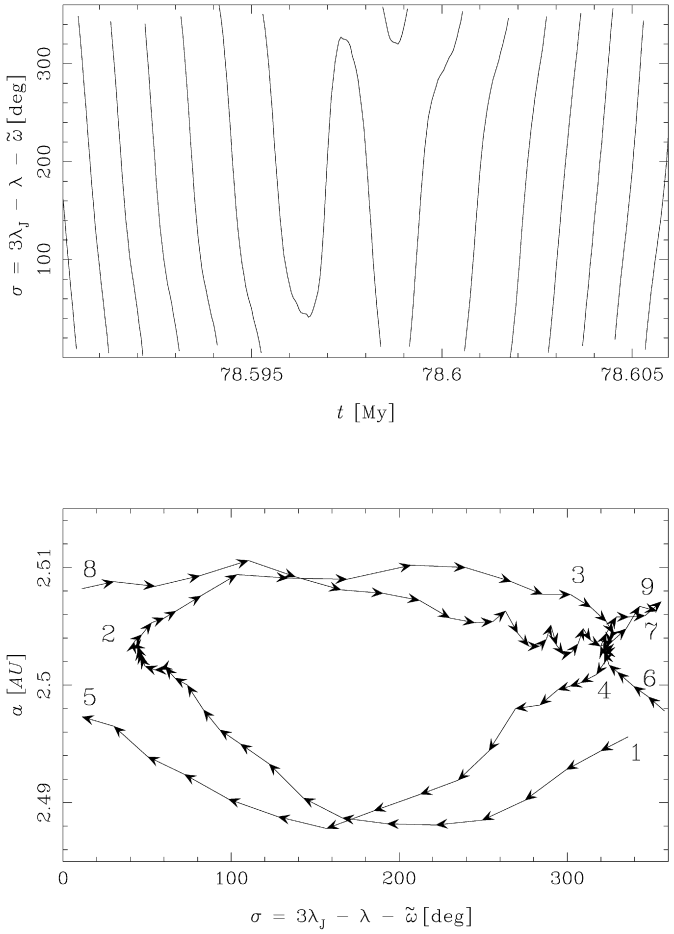

Fig. 4. Detail of the trajectory during the resonance crossing of the slowly drifting test particle shown in Fig. 3. The top panel shows the resonant angle σ as a function of time. The bottom panel shows the trajectory in the space a, σ. The arrows indicate the direction of the trajectory. The numbers provide the temporal sequence of the trajectory.

Table 4
Fraction $f_{\rm cross}$ of asteroids that crossed the J3/1 MMR during our simulations for different Yarkovsky drifts

$da/dt \times 10^{-4}$ [AU/My]	$\sim D$ [km]	$f_{\rm cross}$
1.0 ± 0.1	2.50	0.0033 ± 0.0019
2.5 ± 0.25	1.00	0.0080 ± 0.0028
10.0 ± 1.0	0.25	0.029 ± 0.005

a linear dependence between $f_{\rm cross}$ and da/dt within the studied range of drift rates, and taking into account Eq. (1), we find that

$$f_{\rm cross}(D) \simeq 0.0075 \frac{1\ {\rm km}}{D} \cos\epsilon. \qquad (2)$$

The application of this formula in the size range 1 km $\lesssim D \lesssim$ 5 km requires only modest extrapolations of the linear dependence toward smaller values of the drift rate ($\sim 0.5 \times 10^{-4}$ AU/My). This result demonstrates, for the first time, that the crossing of Vesta family members over the J3/1 MMR is possible in practice. The crossing probability ranges from 0.15 to 0.25% for asteroids in the size range of (21238) and (40521).

4. The production of V-type asteroids with $a > 2.5$ AU

In the preceding section, we have shown that, in practice, it is possible for a former Vesta family member to cross the J3/1 MMR, reaching a stable orbit in the middle belt. We have also estimated the crossing probability as a function of the size (Eq. (2)) to be ~0.1–0.8% for km-size asteroids. We may now wonder whether this may actually explain the presence of (21238) and (40521) in the middle belt.

The number of Vesta family members, with diameters between D and $D + {\rm d}D$, that cross the J3/1 MMR during the age of the Vesta family, $\tau_{\rm age}$, and end in the middle belt is

$${\rm d}N_{a>2.5}(D) = {\rm d}N_0(D)\, f_{\rm col}(D)\, f_{\rm reach}(D)\, f_{\rm cross}(D), \qquad (3)$$

where ${\rm d}N_0(D)$ is the number of Vesta family members that were produced when the family formed. The factor $f_{\rm col}(D)$ accounts for the fraction of Vesta family members in the interval $[D, D + {\rm d}D]$ that, on one hand, survived the collisional evolution untouched and, on the other hand, were created by the collisions during $\tau_{\rm age}$. It is worth noting that the product ${\rm d}N_0(D) f_{\rm col}(D)$ is equivalent to the presently observed number of family members, ${\rm d}N(D)$. The factor $f_{\rm reach}(D)$ accounts for the fraction of Vesta family members that were able to reach the border of the J3/1 MMR in $\tau_{\rm age}$ aided by the Yarkovsky effect. Finally, the factor $f_{\rm cross}(D)$ is provided by Eq. (2). In order to apply Eq. (3), we have to address three main issues.

The first issue concerns the actual age of the Vesta family, $\tau_{\rm age}$. Initial estimates by Marzari et al. (1996), based on collisional evolution models aiming to reproduce the presently observed size frequency distribution of the Vesta family, indicated $\tau_{\rm age} \sim$ 1–2 Gy. However, these estimates have large uncertainties due to unknown initial conditions and to uncertainties in the various collisional parameters. Carruba et al. (2005), based on the dynamical evolution of the V-type Asteroids (956) Elisa and (809) Lundia, give a lower bound of $\tau_{\rm age} \gtrsim 1.2$ Gy. A similar estimate ($\tau_{\rm age} \sim 1.2$ Gy) is given by Carruba et al. (2007b), based on the evolution of V-type asteroids by close encounters with (4) Vesta. On the other hand, Bogard and Garrison (2003), measuring isotopic abundances in the Howardite–Eucrite–Diogenite (HED) meteorites—that presumably come from Vesta (Migliorini et al., 1997)—concluded that Vesta's crust suffered several major craterization impacts $\gtrsim$3.5 Gy ago. This could imply $\tau_{\rm age} \gtrsim 3.5$ Gy (but $\lesssim$3.9 Gy because asteroid families would probably not have survived to the epoch of the Late Heavy Bombardment, e.g., Gomes et al., 2005). In view of the wide range of possible ages, we will adopt for our calculations three different values of $\tau_{\rm age}$: 1.5, 2.5 and 3.5 Gy.

The second issue to address is to estimate the fraction of family members, $f_{\rm reach}$, that would be able to reach the J3/1 MMR in $\tau_{\rm age}$ due to the Yarkovsky effect. For this purpose, we used a Monte Carlo algorithm. We generated an artificial Vesta family constituted of 10,000 fragments with individual ejection velocities, $v_{\rm ej}$, attributed by assuming a Maxwellian distribu-

tion with mean ejection velocity $\bar{v}_{ej}$.[6] We considered only the fragments with

$$v_{ej}^2 - v_{esc}^2 > 0 \quad \text{and} \quad v_{ej}^2 - v_{cut}^2 < 0,$$

where $v_{esc} = 314$ m/s is the escape velocity from the surface of (4) Vesta,[7] and $v_{cut} = 600$ m/s is a maximum cutoff velocity (Asphaug, 1997). We further assumed that, at the moment of the impact, (4) Vesta had a true anomaly and perihelion argument such that the final distribution of the fragments in proper elements space is spread over a wide range of a_p, e_p, I_p (Morbidelli et al., 1995), as observed. Finally, we considered that all the fragments had the same diameter—i.e., the ejection velocity does not depend on size—and attributed to each fragment a random value of $\cos\epsilon$ between -1 and 1. Using Eq. (1), we computed for each fragment the total drift over τ_{age} and determined the fraction f_{reach} that ended with $a > 2.5$ AU. Neither the collisional reorientations of spin axes nor the YORP effect were taken into account in this model. Both these effects depend on several parameters with largely uncertain values, thus their precise modeling is difficult. The possible consequences of disregarding these effects will be addressed later in this section.

Fig. 5 shows $f_{reach}(D)$ as a function of τ_{age} and of plausible values of $\bar{v}_{ej}$ (Asphaug, 1997). For very small sizes, f_{reach} weakly depends on $\bar{v}_{ej}$ and tends to 50% for $D \to 0$. This means that about half of the smallest fragments will eventually reach the J3/1 MMR (the other half has $\cos\epsilon < 0$ so is drifting inwards). On the other hand, for very large sizes $f_{reach} \to 0$ since large bodies have much smaller Yarkovsky semi-major axis drifts. It is worth noting that size range where the behavior of f_{reach} is more critical, i.e., more sensitive to the different parameters and especially to the family age, is between 2.0 and 7.0 km, which is precisely the size range of the asteroids we are interested in (see Table 1).

The third issue to address concerns the determination of the size frequency distribution (SFD), $dN(D)$, of the Vesta family. The Vesta family, as defined by the HCM (Section 3), shows a very distinct SFD. Going from larger to smaller sizes, we first find (4) Vesta with $D \sim 460$ km. Then we find four asteroids with $25 \lesssim D \lesssim 130$ km and twelve asteroids with $8 \lesssim D \lesssim 15$ km, which taxonomic types, based on spectroscopic observations (Bus and Binzel, 2002a; Lazzaro et al., 2004), are different from the V-type. These asteroids are interlopers in the family and we can exclude them. Finally, we find a huge amount of members with $D < 8$ km. This group includes all the Vestoids, i.e., the known V-type asteroids that are members of the Vesta family. According to simulations of asteroid fragmentation using hydrocodes (Durda et al., 2007), this kind of SFD, with one large asteroid and a huge amount of very small fragments with no bodies in between, would be typical

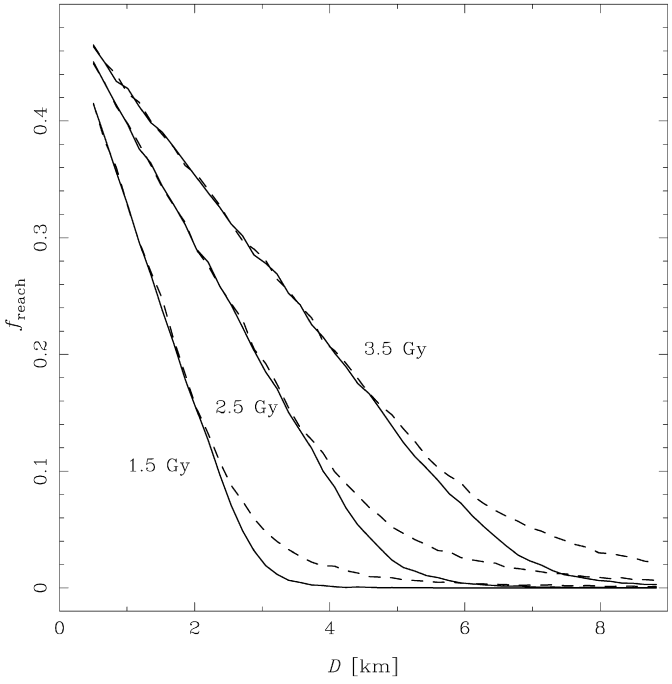

Fig. 5. The fraction f_{reach} of Vesta's fragments that reached the J3/1 MMR border along three different values of τ_{age}, and for two different values of $\bar{v}_{ej}$: 150 m/s (full lines) and 300 m/s (dashed lines).

of craterization events as the one(s) that presumably formed the Vesta family.

Now, $dN(D)$ is related to the differential SFD, $n(D)$, through

$$dN(D) = n(D)\,dD$$

and the cumulative SFD, i.e., the number of family members with diameter $> D$, is given by

$$N(>D) = \int_D^{D_{max}} n(D)\,dD, \tag{4}$$

where D_{max} is the size of the largest family member (i.e., (4) Vesta). Fig. 6 shows the cumulative SFD of the Vesta family after removing the known interlopers. For $D < 8$ km the cumulative SFD can be fit by a broken power law of the form $N_0 D^{\gamma}$ (dashed lines in Fig. 6), where γ and N_0 have different values in different size ranges. This change in γ and N_0 is produced by two different effects:

1. The fact that the sample of known family members is complete only up to a given size. It is usually assumed that this completeness limit corresponds to the size where the cumulative SFD shows the first inflexion point from the right (e.g., Tanga et al., 1999), which is 5.5 km in Fig. 6, but this assumption may not be applicable to all cases and the actual completeness limit could be at smaller sizes.
2. The natural dynamical/collisional evolution of the family members, which is known to produce a shallow cumulative SFD at small sizes (Morbidelli et al., 2003).

[6] We recall that the specific energy of the impact that generated the family is $\propto \bar{v}_{ej}^2$.

[7] $v_{esc} = \sqrt{1.64\, G\, \frac{4}{3}\pi\rho R^2}$ being R the radius of Vesta and ρ its density (Petit and Farinella, 1993)

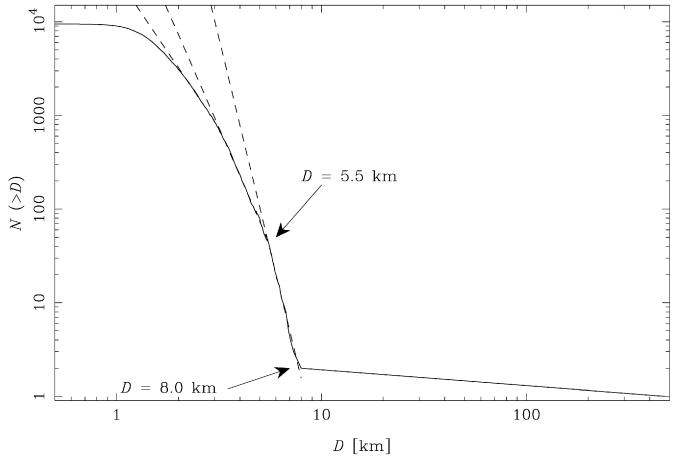

Fig. 6. The cumulative size distribution of the Vesta family after subtracting the known interlopers (full line) and three power law fits for different size ranges (dashed lines). Diameters were computed assuming albedo 0.4 for all bodies.

Since both these effects are difficult to estimate, we will adopt here two limiting cases of the cumulative SFD of the Vesta family:

- A lower limit represented by the observed cumulative SFD as shown in Fig. 6. This approach partly accounts for effect #2, but has the drawback that it will be biased by the incompleteness of the sample at the small sizes.
- An upper limit represented by a single power law fit between 8 and 5.5 km, extrapolated to smaller sizes. This approach partly accounts for effect #1, but has the drawback that it will significantly overestimate the number of small members in the Vesta family, especially in the size range 2.0–5.5 km that is crucial for our study. With this approach, the differential SFD will also be modeled by a single power law of the form $n_0 D^{\gamma-1}$.

Knowing all the quantities involved in Eq. (3), it is now possible to determine the number of Vesta family members with size $>D$ that cross the J3/1 MMR and reach the middle belt in $\tau_{\rm age}$:

$$N_{a>2.5}(>D) = \int_{D}^{D'_{\rm max}} n(D)\, f_{\rm reach}(D)\, f_{\rm cross}(D)\, {\rm d}D, \qquad (5)$$

This integral can be solved numerically taking into account that $D'_{\rm max} = 8$ km. The results are shown in Fig. 7 for $\bar{v}_{\rm ej} = 200$ m/s and three different values of $\tau_{\rm age}$. The full lines were obtained using the observed SFD (lower limit), and the dashed lines using the single power law fit of the SFD (upper limit). The true value of $N_{a>2.5}$ $(>D)$, for a given $\tau_{\rm age}$, should lie somewhere in between the corresponding full and dashed lines.

From Fig. 7, it is clear that the predicted $N_{a>2.5}$ for $D \gtrsim$ 5 km is at least two orders of magnitude smaller than required to produce a body like (21238). Therefore, we may conclude that, even if the crossing over the J3/1 MMR is dynamically possible, it is highly improbable that (21238) had reached its present orbit via this mechanism. On the other hand, for $D \gtrsim$

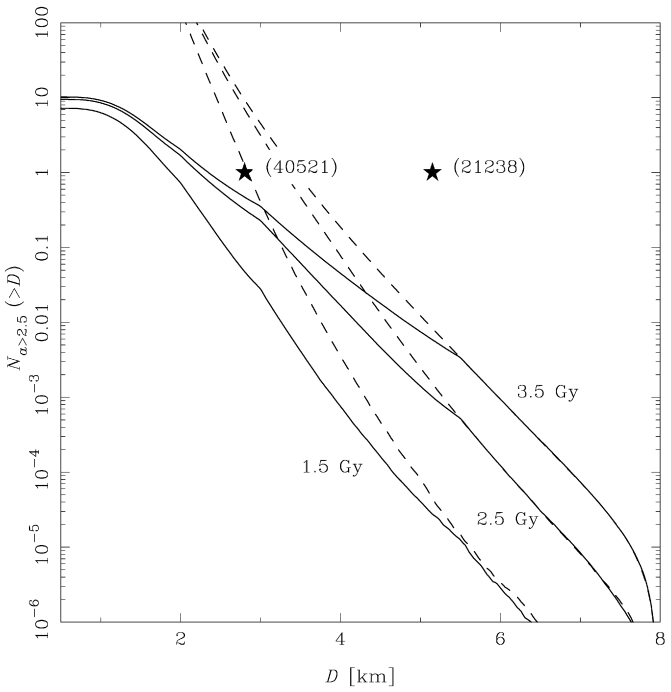

Fig. 7. The cumulative distribution $N_{a>2.5}$ for three different values of $\tau_{\rm age}$ and two limiting cases of the SFD: the observed SFD (full lines) and the single power law SFD (dashed lines). In all cases $\bar{v}_{\rm ej} = 200$ m/s. The stars represent the known V-type asteroids in the middle belt.

3 km the predicted $N_{a>2.5}$ is compatible with the presence of (40521) in the middle belt, provided that $\tau_{\rm age} \gtrsim 3.5$ Gy.

We must recall that the above results have been obtained by assuming that our test particles do not change their spin axes orientation during the whole evolution. This is not the real case and we should expect the spin axes to change due to collisions (Harris, 1979) and to the YORP effect (Rubincam, 2000). In the former case, it is expected that non-disruptive collisions would be able to reorient the spin axis of a small body from prograde to retrograde, or vice versa, thus causing a delay in the arrival time of the asteroids to the border of the J3/1 MMR. It is usually *assumed* that collisional reorientations happen in a random way with a certain characteristic timescale that depends on the asteroid's size, so smaller bodies reorient more frequently. For km-size asteroids typical timescales range from 100 My to 1 Gy (e.g., Farinella et al., 1998). By including random reorientations in our model, we verified that the more the asteroid reorients, the longer the time it takes to reach the 3/1 resonance. We estimated that the fraction $f_{\rm reach}$ shown in Fig. 5 decays by a factor of $\sim 2/3$ at a size of $\sim$1 km.

On the other hand, the YORP effect statistically tends to align the spin axes around $\epsilon \sim 0, \pi$, thus forcing an increase of the Yarkovsky drift, on average, for all the particles. Bottke et al. (2006) suggest that the YORP effect might be more important than collisional reorientations in governing the evolution of asteroids' spin axes, then we may expect that it partially compensates the delay caused by collisional reorientations. Unfortunately, this is difficult to quantify precisely. Roughly speaking, we can say that the estimates presented in Figs. 5 and 7 probably represent an upper limit and they should be multiplied

by some factor between ∼0.7 and 1. Even so, our model is still compatible with the presence of (40521) in the middle belt.

5. Predicted vs observed number of V-type asteroids in the middle belt

Our results above have been compared to the observed population of V-type asteroids in the middle belt, which is most likely incomplete. Here we will estimate the debiased SFD of V-type asteroids in the region $2.5 < a \lesssim 2.6$ AU, where (21238) and (40521) are located, and will compare it to our estimates of $N_{a>2.5}$.

In terms of the absolute magnitude H, the unbiased differential SFD of V-type asteroids in the region of interest, $n_{\rm V}(H)\,{\rm d}H$, is related to the observed differential SFD, $n_{\rm V}^{\rm obs}(H)\,{\rm d}H$, through

$$n_{\rm V}^{\rm obs}(H)\,{\rm d}H = b(H) n_{\rm V}(H)\,{\rm d}H, \tag{6}$$

where $b(H)$ is a bias function that we need to determine. This bias function arises from two main effects: (i) the fact that the known population of asteroids is complete only up to a certain size, and (ii) the fact that the observed population $n_{\rm V}^{\rm obs}$ is obtained from the SDSS that mapped only a fraction of the total known population of asteroids. We may assume that effect (i) affects the asteroid populations at both sides of the J3/1 MMR approximately in the same way (because the heliocentric distance is almost the same), so it can be ignored in our analysis. From effect (ii), we have that

$$b(H) \simeq \frac{n_{\rm SDSS}(H)\,{\rm d}H}{n_{\rm know}(H)\,{\rm d}H}, \tag{7}$$

where $n_{\rm SDSS}\,{\rm d}H$ is the SFD of asteroids with $2.5 < a \lesssim 2.6$ AU contained in the 3rd release of the SDSS-MOC, and $n_{\rm know}\,{\rm d}H$ is the SFD of all the known asteroids in the same region, that can be computed from the catalog of proper elements contemporary to the SDSS-MOC. Fig. 8 shows $b(H)$ (full line) and its best fit (dashed line). The bias shows a linear dependence for $H \gtrsim 13.0$, and a constant value ∼0.22 for $H \lesssim 13.0$.

The observed SFD $n_{\rm V}^{\rm obs}$ is poorly known since, according to Table 1, there are only two asteroids observed by the SDSS-MOC in the range $2.5 < a \lesssim 2.6$ AU. Notwithstanding, we can use additional observations from the SDSS-MOC to get a more populated SFD. We follow the same approach as Roig and Gil-Hutton (2006) to identify V-type asteroids from the SDSS-MOC, but we disregard the information in the u band. This is justified since the u band is centered at ≃0.35 μm and it is not relevant for the identification of V-type asteroids. Thus, we considered the SDSS-MOC observations with errors less than 10% only in the g, r, i, z bands and with any error in the u band. With this approach, we find 24 V-type candidates in the middle belt, besides the three asteroids listed in Table 1. These new candidates are listed in Table 5.

The cumulative SFD of the 10 V-type candidates identified in the region $2.5 < a \lesssim 2.6$ AU, and the corresponding debiased cumulative SFD computed from Eqs. (6) and (7), are shown in Fig. 9 (full lines). It is worth recalling that both SFDs are affected by the completeness bias of the known asteroidal

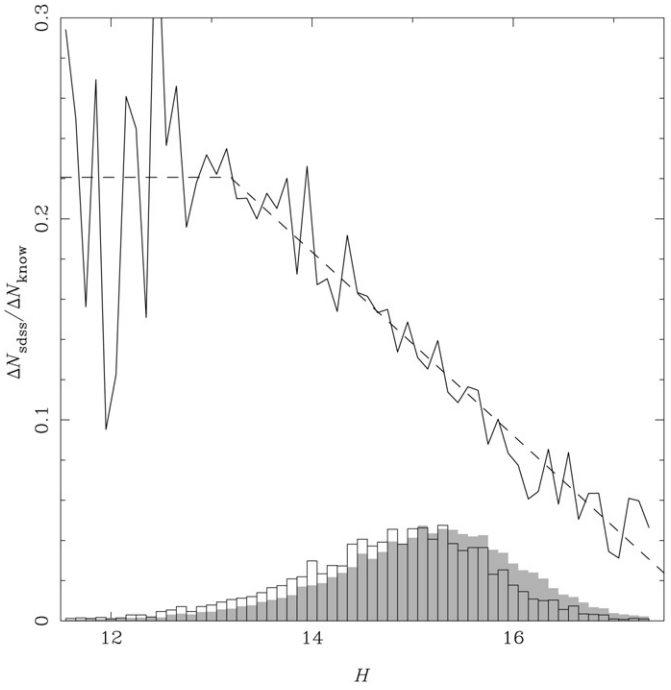

Fig. 8. The bias function (full line) in the region $2.5 < a \lesssim 2.6$ AU, and its best fit (dashed line). The distributions $n_{\rm know}\Delta H$ (gray histogram) and $n_{\rm sdss}\Delta H$ (outlined histogram) are shown for reference. Both distributions are normalized such that $\sum n\Delta H = 1$.

Table 5
Same parameters as in Table 1 for the 24 candidate V-type asteroids in the middle belt, predicted from the colors of the SDSS-MOC by relaxing the selection criteria (see text)

Name	a_p [AU]	e_p	$\sin I_p$	H	D [km]
(10800) 1992OM8	2.54967	0.0924	0.0217	14.12	3.15
(24574) 3312T-1	2.64529	0.0697	0.0370	14.88	2.22
(28582) 2000EB106	2.75282	0.1180	0.2205	13.49	4.21
(29300) 1993TD25	2.53865	0.1437	0.0484	15.09	2.02
(31534) 1999CE149	2.59211	0.1146	0.0279	14.90	2.20
(41446) 2000LW	2.77435	0.1266	0.1571	13.85	3.57
(44204) 1998MJ35	2.54207	0.1507	0.1987	14.14	3.12
(48558) 1993TL38	2.76241	0.1386	0.0890	13.85	3.57
(57439) 2001SJ53	2.56172	0.0677	0.0629	14.82	2.28
(62002) 2000RT37	2.75865	0.2264	0.4357	14.08	3.21
(68538) 2001VN125	2.77037	0.1362	0.0875	14.90	2.20
(75952) 2000CD91	2.68370	0.1379	0.0675	14.90	2.20
(87110) 2000LW21	2.71120	0.1606	0.2390	14.33	2.86
(93322) 2000SA221	2.74323	0.0990	0.2080	14.40	2.77
(110005) 2001SH64	2.67299	0.1067	0.1611	14.79	2.31
(110891) 2001UD113	2.62939	0.0975	0.0703	14.70	2.41
(113194) 2002RY107	2.72062	0.1037	0.1646	14.42	2.74
(119686) 2001XY116	2.71507	0.1797	0.1632	14.84	2.26
(121046) 1999CD34	2.52253	0.1289	0.0478	15.95	1.36
(126836) 2002EP64	2.60219	0.2627	0.1123	15.82	1.44
2001TG179	2.71855	0.0386	0.1063	15.92	1.38
2001UY185	2.78548	0.0857	0.1600	16.10	1.27
2003UE237	2.67057	0.0810	0.1573	15.55	1.63
4089T-2	2.54502	0.1691	0.0512	16.23	1.19

It is worth noting that up to 70% of the candidates in this list might not be V-type asteroids.

population with $a > 2.5$ AU. Therefore, we may compare these distributions to our lower limit predictions of $N_{a>2.5}$, computed from the observed Vesta family SFD which are affected by

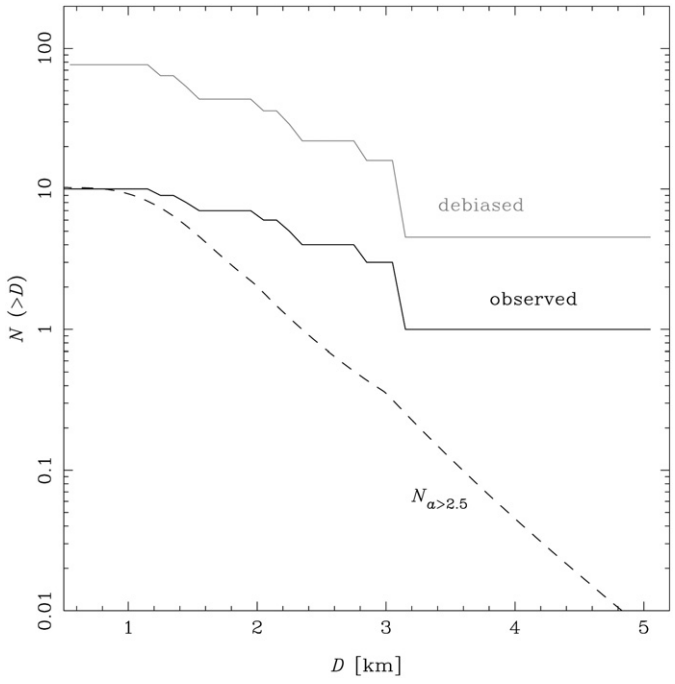

Fig. 9. The cumulative SFD of V-type asteroids with $2.5 < a \lesssim 2.6$ AU observed by the SDSS (full black line) and the corresponding debiased distribution (full gray line). The dashed line represents our predicted $N_{a>2.5}$ for $\tau_{\rm age} = 3.5$ Gy, computed from the observed SFD of the Vesta family.

about the same completeness bias. The comparison to $N_{a>2.5}$ for $\tau_{\rm age} = 3.5$ Gy (dashed line in Fig. 9) indicates that the predictions are $\gtrsim$10 times smaller than required in the studied size range. However, we must bear in mind that the cumulative SFDs shown in Fig. 9 correspond to asteroids that are candidate V-type according to the SDSS colors. An unknown fraction up to ∼70% of these bodies might not be true V-types, but belong to other taxonomic classes like O-, Q-, R- or S-type. Therefore, our predictions could actually account for 10 to 30% of the total population of V-type asteroids with $D > 1$ km in the middle belt, assuming $\tau_{\rm age} \gtrsim 3.5$ Gy. Smaller values of $\tau_{\rm age}$ are not compatible with our scenario, *thus putting a constraint to the age of the Vesta family*.

6. Conclusions

In this paper, we presented spectroscopic observations in the visible that confirm the existence of two V-type asteroids in the middle belt: (21238) 1995WV7 and (40521) 1999RL95. We investigate whether these two asteroids might have evolved from the Vesta family by slowly drifting in semi-major axis due to the Yarkovsky effect and crossing over the J3/1 mean motion resonance with Jupiter. Our results show that, in spite of the remarkable instability of the J3/1 resonance, km-size asteroids can cross it, albeit with a low probability. The resonance crossing mechanism is probably not sufficiently efficient to explain the presence of all km-size V-type asteroids in the middle belt, but only some 10 to 30% fraction constituted of the small ones, like (40521). The other 70 to 90% bodies either followed other dynamical paths from the Vesta family—e.g., combining planetary close encounters and resonance capture (Roig et al., 2007), or during the epoch of the planetary migration (see discussion in Nesvorný et al., 2008)—or they come from a totally different source, e.g., the Eunomia family (Carruba et al., 2007a). Notwithstanding, we cannot rule out the possibility that (21238) were a rare exception: the only one 5-km V-type asteroid in the middle belt that reached its present orbit by a *highly improbable, but not impossible*, crossing over the J3/1 resonance. Only the discovery of more V-type asteroids in the middle belt, and a better knowledge of the SFD of these bodies may shed some light on this problem.

Acknowledgments

We wish to thank the referees Mira Broz and Valerio Carruba for their helpful criticism and suggestions. This work has been supported through several grants and fellowships by the Brazilian Council of Research (CNPq), the NASA's Planetary Geology & Geophysics Program, and the Rio de Janeiro State Science Foundation (FAPERJ).

References

Asphaug, E., 1997. Impact origin of the Vesta family. Meteorit. Planet. Sci. 32, 965–980.

Binzel, R.P., Masi, G., Foglia, S., 2006. Prediction and confirmation of V-type asteroids beyond 2.5 AU based on SDSS colors. Bull. Am. Astron. Soc. 38, 627.

Bogard, D.D., Garrison, D.H., 2003. 39Ar–40Ar ages of eucrites and thermal history of Asteroid 4 Vesta. Meteorit. Planet. Sci. 38, 669–710.

Bottke Jr., W.F., Vokrouhlický, D., Rubincam, D.P., Nesvorný, D., 2006. The Yarkovsky and Yorp effects: Implications for asteroid dynamics. Annu. Rev. Earth Planet. Sci. 34, 157–191.

Bus, S.J., Binzel, R.P., 2002a. Phase II of the Small Main-Belt Asteroid Spectroscopic Survey: A feature-based taxonomy. Icarus 158, 146–177.

Bus, S.J., Binzel, R.P., 2002b. Phase II of the Small Main-Belt Asteroid Spectroscopic Survey: The observations. Icarus 158, 106–145.

Carruba, V., Michtchenko, T.A., Roig, F., Ferraz-Mello, S., Nesvorný, D., 2005. On the V-type asteroids outside the Vesta family. I. Interplay of non-linear secular resonances and the Yarkovsky effect: The cases of 956 Elisa and 809 Lundia. Astron. Astrophys. 441, 819–829.

Carruba, V., Michtchenko, T.A., Lazzaro, D., 2007a. On the V-type asteroids outside the Vesta family. II. Is (21238) 1995 WV7 a fragment of the long-lost basaltic crust of (15) Eunomia? Astron. Astrophys. 473, 967–978.

Carruba, V., Roig, F., Michtchenko, T.A., Ferraz-Mello, S., Nesvorný, D., 2007b. Modeling close encounters with massive asteroids: A Markovian approach, an application to the Vesta family. Astron. Astrophys. 465, 315–330.

Delbo, M., Gai, M., Lattanzi, M.G., Ligori, S., Loreggia, D., Saba, L., Cellino, A., Gandolfi, D., Licchelli, D., Blanco, C., Cigna, M., Wittkowski, M., 2006. MIDI observations of 1459 Magnya: First attempt of interferometric observations of asteroids with the VLTI. Icarus 181, 618–622.

Duffard, R., Roig, F., 2007. Two new basaltic asteroids in the outer Main Belt. ArXiv e-print, astro-ph/0704.0230.

Durda, D.D., Bottke, W.F., Nesvorný, D., Enke, B.L., Merline, W.J., Asphaug, E., Richardson, D.C., 2007. Size frequency distributions of fragments from SPH/N-body simulations of asteroid impacts: Comparison with observed asteroid families. Icarus 186, 498–516.

Farinella, P., Vokrouhlicky, D., Hartmann, W.K., 1998. Meteorite delivery via Yarkovsky orbital drift. Icarus 132, 378–387.

Gladman, B.J., Migliorini, F., Morbidelli, A., Zappalà, V., Michel, P., Cellino, A., Froeschlé, C., Levison, H.F., Bailey, M., Duncan, M., 1997. Dynamical lifetimes of objects injected into asteroid belt resonances. Science 277, 197–201.

Gomes, R., Levison, H.F., Tsiganis, K., Morbidelli, A., 2005. Origin of the cataclysmic late heavy bombardment period of the terrestrial planets. Nature 435, 466–469.

Hammergren, M., Gyuk, G., Puckett, A., 2006. (21238) 1995 WV7: A new basaltic asteroid outside the 3:1 mean motion resonance. ArXiv e-print, astro-ph/0609420.

Harris, A.W., 1979. Asteroid rotation rates. II. A theory for the collisional evolution of rotation rates. Icarus 40, 145–153.

Ivezić, Ž, Tabachnik, S., Rafikov, R., Lupton, R.H., Quinn, T., Hammergren, M., Eyer, L., Chu, J., Armstrong, J.C., Fan, X., Finlator, K., Geballe, T.R., Gunn, J.E., Hennessy, G.S., Knapp, G.R., Leggett, S.K., Munn, J.A., Pier, J.R., Rockosi, C.M., Schneider, D.P., Strauss, M.A., Yanny, B., Brinkmann, J., Csabai, I., Hindsley, R.B., Kent, S., Lamb, D.Q., Margon, B., McKay, T.A., Smith, J.A., Waddel, P., York, D.G., and the SDSS Collaboration, 2001. Solar System objects observed in the Sloan Digital Sky Survey Commissioning data. Astron. J. 122, 2749–2784.

Landolt, A.U., 1992. UBVRI photometric standard stars in the magnitude range 11.5–16.0 around the celestial equator. Astron. J. 104, 340–371.

Lazzaro, D., Michtchenko, T., Carvano, J.M., Binzel, R.P., Bus, S.J., Burbine, T.H., Mothé-Diniz, T., Florczak, M., Angeli, C.A., Harris, A.W., 2000. Discovery of a basaltic asteroid in the outer Main Belt. Science 288, 2003–2035.

Lazzaro, D., Angeli, C.A., Carvano, J.M., Mothé-Diniz, T., Duffard, R., Florczak, M., 2004. S^3OS^2: The visible spectroscopic survey of 820 asteroids. Icarus 172, 179–220.

Levison, H.F., Duncan, M.J., 1994. The long-term dynamical behavior of short-period comets. Icarus 108, 18–36.

Marzari, F., Cellino, A., Davis, D.R., Farinella, P., Zappalà, V., Vanzani, V., 1996. Origin and evolution of the Vesta asteroid family. Astron. Astrophys. 316, 248–262.

McCord, T.B., Adams, J.B., Johnson, T.V., 1970. Asteroid Vesta: Spectral reflectivity and compositional implications. Science 168, 1445–1447.

Michtchenko, T.A., Lazzaro, D., Ferraz-Mello, S., Roig, F., 2002. Origin of the basaltic Asteroid 1459 Magnya: A dynamical and mineralogical study of the outer Main Belt. Icarus 158, 343–359.

Migliorini, F., Morbidelli, A., Zappalà, V., Gladman, B.J., Bailey, M.E., Cellino, A., 1997. Vesta fragments from v6 and 3:1 resonances: Implications for V-type NEAs and HED meteorites. Meteorit. Planet. Sci. 32, 903–916.

Morbidelli, A., Zappalà, V., Moons, M., Cellino, A., Gonczi, R., 1995. Asteroid families close to mean motion resonances: Dynamical effects and physical implications. Icarus 118, 132–154.

Morbidelli, A., Nesvorný, D., Bottke, W.F., Michel, P., Vokrouhlický, D., Tanga, P., 2003. The shallow magnitude distribution of asteroid families. Icarus 162, 328–336.

Moskovitz, N.A., Willman, M., Lawrence, S.J., Jedicke, R., Nesvorný, D., Gaidos, E.J., 2007. A survey of basaltic asteroids in the Main Belt. Lunar Planet. Sci. 38, 1663–1664.

Mothé-Diniz, T., Roig, F., Carvano, J.M., 2005. Reanalysis of asteroid families structure through visible spectroscopy. Icarus 174, 54–80.

Nathues, A., Mottola, S., Kaasalainen, M., Neukum, G., 2005. Spectral study of the Eunomia asteroid family. Icarus 175, 452–463.

Nesvorný, D., Roig, F., Lazzaro, D., Gladman, B., Carruba, V., 2008. Fugitives from the Vesta family. Icarus 193, 85–95.

Petit, J.-M., Farinella, P., 1993. Modeling the outcomes of high-velocity impacts between small Solar System bodies. Celest. Mech. Dynam. Astron. 57, 1–2.

Roig, F., Gil-Hutton, R., 2006. Selecting candidate V-type asteroids from the analysis of the Sloan Digital Sky Survey colors. Icarus 183, 411–419.

Roig, F.V., Nesvorný, D., Gladman, B., Gil-Hutton, R., Lazzaro, D., Carruba, V., Mothé-Diniz, T., 2007. Origin of basaltic asteroids in the main asteroid belt. Bul. Am. Astron. Soc. 39. Abstract #50.05.

Rubincam, D.P., 1995. Asteroid orbit evolution due to thermal drag. J. Geophys. Res. 100, 1585–1594.

Rubincam, D.P., 2000. Radiative spin-up and spin-down of small asteroids. Icarus 148, 2–11.

Tanga, P., Cellino, A., Michel, P., Zappalà, V., Paolicchi, P., dell'Oro, A., 1999. On the size distribution of asteroid families: The role of geometry. Icarus 141, 65–78.

Tedesco, E.F., 1989, Asteroid magnitudes, UBV colors, and IRAS albedos and diameters. In: Binzel, R.P., Gehrels, T., Matthews, M.S. (Eds.). Asteroids II. Univ. of Arizona Press, Tucson, pp. 1090–1138.

Tholen, D.J., 1989. Asteroid taxonomic classifications. In: Binzel, R.P., Gehrels, T., Matthews, M.S. (Eds.). Asteroids II. Univ. of Arizona Press, Tucson, pp. 1139–1150.

Thomas, P.C., Binzel, R.P., Gaffey, M.J., Storrs, A.D., Wells, E.N., Zellner, B.H., 1997. Impact excavation on Asteroid 4 Vesta: Hubble Space Telescope results. Science 277, 1492–1495.

Vokrouhlický, D., 1999. A complete linear model for the Yarkovsky thermal force on spherical asteroid fragments. Astron. Astrophys. 344, 362–366.

Vokrouhlický, D., Milani, A., Chesley, S.R., 2000. Yarkovsky effect on small near-Earth asteroids: Mathematical formulation and examples. Icarus 148, 118–138.

Wisdom, J., 1982. The origin of the Kirkwood gaps—A mapping for asteroidal motion near the 3/1 commensurability. Astron. J. 87, 577–593.

Zappalà, V., Cellino, A., Farinella, P., Knežević, Z., 1990. Asteroid families. I. Identification by hierarchical clustering and reliability assessment. Astron. J. 100, 2030–2046.